3.5.4 ICRS Centre

The International Earth Rotation and Reference System (IERS) International Celestial Reference System (ICRS) Centre is tasked with the maintenance of the International Celestial Reference System (ICRS) and the International Celestial Reference Frame (ICRF) for the international astronomical and geodesy communities. Responsibilities are shared jointly between Paris Observatory (PO) and the U.S. Naval Observatory (USNO). Critical ICRS and ICRF-relevant activities from 2018 are described for both OP and USNO in the following sections.

Paris Observatory IERS ICRS Centre Activities During 2018

Construction of the ICRF3

Staff of the ICRS Centre at Paris Observatory worked on the construction of the Third Realization of the International Celestial Reference Frame (ICRF3) in the frame of activities of the Working Group on ICRF3 created at the XXVIII IAU General Assembly in 2012. The mission of the WG-ICRF3 concluded with the proposal to and adoption by the XXX IAU General Assembly in August 2018 of a catalog of radio source positions which realize the ICRS (Charlot et al. 2020). Resolution B2 of the XXX IAU General Assembly (IAU 2019) resolves that as from 1 January 2019 ICRF3 is the fundamental realization of the International Celestial Reference System (ICRS). The ICRF3 is aligned onto ICRF2 (Fey et al. 2015) and represents a significant improvement in terms of radio source characterization, position accuracy and total number of sources. Objects in the new frame had been used to orientate the Gaia DR2 catalog onto the ICRS, as will be the case of the Gaia final catalog.

The ICRF3 is represented by three catalogs at bands S/X, K and X/Ka with 4536, 824 and 678 objects respectively (http://iers.obspm.fr/icrs-pc/newwww/icrf).

Monitoring of the ICRS

Monitoring the ICRS is a mission of the IERS ICRS Centre. This includes verifications of the stability of the axes of the system materialized though the frame, identification of the possible deformations of the frame and tracking the astrometric evolution of its defining sources. Another aspect of this activity consists on the analysis of individual solutions submitted by the VLBI analysis centres to the International VLBI Service (IVS).

The IERS ICRS Centre at Paris Observatory developed the tools for determining the orientation of the axes, characterizing the deformations of the frame and analyzing the astrometric quality of radio source positions (Lambert 2013). Until mid-2018 these analyses were focused on the monitoring of the defining sources of the ICRF2 and contributed to selection of the defining sources of ICRF3.

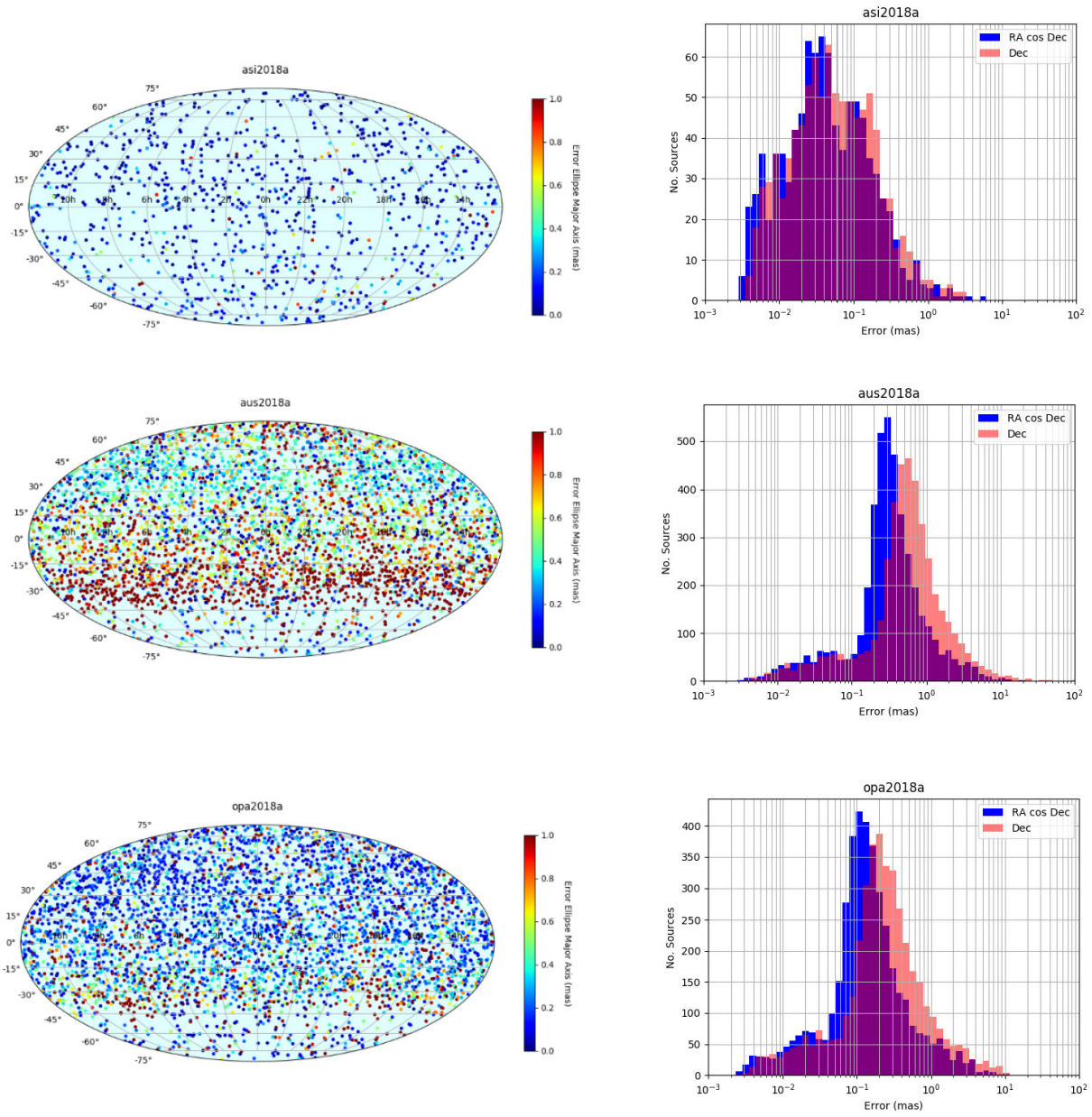

Fig. 1: *Left: sky distribution of the catalogs highlighting the overall positional error computed as the major axis of the error ellipse. Right: distribution of the standard errors on source position.*

Analysis of recent VLBI catalogs

Data

We analyzed three catalogs submitted to the International VLBI Service for Geodesy and Astrometry (IVS) in 2018. The catalogs were respectively submitted by the Space Geodesy Centre of the Italian Space Agency (ASI/CGS; solution asi2018a), by Geoscience Australia (aus2018a) and by Paris Observatory (opa2018a). The aus2018a catalog was obtained with the OCCAM geodetic VLBI analysis software package (Titov et al. 2004), whereas the other two catalogs were obtained with Calc/Solve (Ma et al. 1986).

Since the catalogs were released before the date of adoption of the ICRF3, their individual frames had been oriented on ICRF2. However, in our analysis we have compared them to ICRF2 and to the catalog representing ICRF3 in the S/X bands (ICRF3X in this report). The second Gaia data release (DR2; Prusti et al. 2016; Brown et al. 2016, 2018; Mignard et al. 2018) has been used also as a reference for comparison.

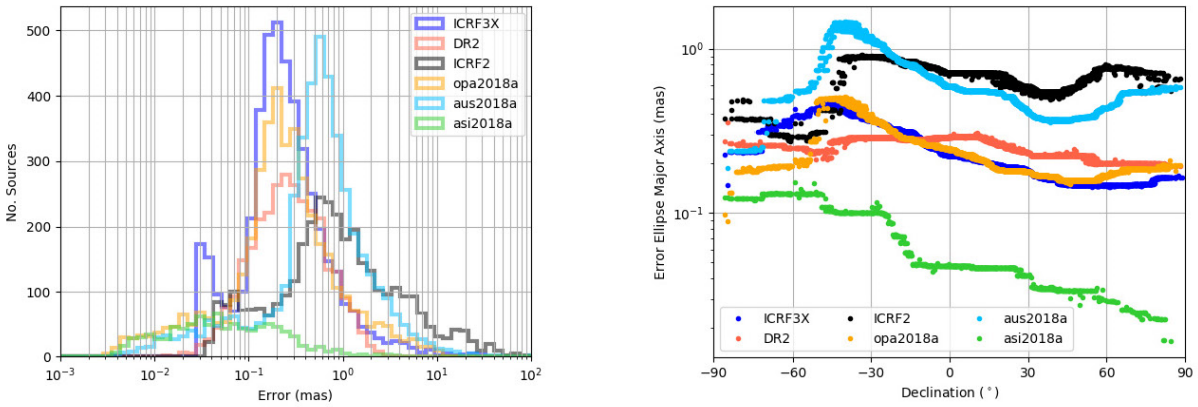

Fig. 2: *Left: overall comparison of the standard error distribution. Right: standard errors in source positions as a function of the declination smoothed by taking the running median within bins of 15 degrees.*

Overview of the catalogs The number of sources in each catalog, the mean epoch of the observations, and the median positional errors (for RA cos DEC, Dec, and for the error ellipse major axis) are reported in Table 1. The ASI solution contains the smallest number of sources. However, these are sources that have the best positional errors, and in consequence the median standard error is neatly smaller than that for the other catalogs. The standard error of the AUS positions is larger than that of OPA in a factor of 2.

Table 1: *Statistic information of the catalogs here reported. N is the number of sources. The mean epoch corresponds to the average of the mean observational epochs of each source. N is the number of sources, E_RA*, E_Dec are respectively the median standard errors in right ascension (scaled by cos dec) and in declination, E_EEMA is the median major axis of error ellipses. Unit is μas.*

	N	Epoch	E_RA*	E_Dec	E_EEMA
opa2018a	4160	2009.24	128.13	216.75	218.07
aus2018a	4267	2009.72	313.24	551.00	554.66
asi2018a	944	2009.24	39.36	48.40	49.48

The sky distribution of the radio sources in each catalog is plotted in Figure 1 together with the distribution of the standard errors. In the sky

maps, the color indicates the overall error computed as the major axis of the error ellipse, calculated using the correlation information between the coordinates as provided in the catalogs.

The error distribution, including that of the catalogs used as reference in the comparisons (ICRF2, ICRF3X and Gaia DR2) and the dependence of the error on the declination are displayed in Figure 2, for which we took the running median error within windows of 15 degrees.

Figure 2 shows a clear declination-dependent error for the individual catalogs and reflects the parameters of Table 1. Both AUS and ASI solutions show larger errors at mid- latitudes in the southern hemisphere, very probably due to the network asymmetry and the lower number of observations in the south. The OPA solution presents a smoother deformation, almost in coincidence with that of ICRF3X. The improvement of ICRF3 with respect of ICRF2 is visible on the plots, both in precision and deformation. The Gaia DR2 solution does not show such systematic effects (the Gaia scanning law allows to cover both hemispheres symmetrically).

Comparison with ICRF2, ICRF3 and Gaia DR2

Figure 3 displays the differences in declination between the catalogs and the references averaged within bins of 15 degrees. All three catalogs share the common feature of large (0.1-mas level) zonal differences with the ICRF2. A similar comparison with Gaia DR2 reveals that for ASI and OPA solutions the zonal deformation is much smaller, which is not the case for the AUS catalog. The same conclusion is valid for the zonal differences with respect to ICRF3X. Since Gaia DR2 is not expected to present zonal deformations, Figure 3 suggests that recent VLBI catalogs are less deformed than ICRF2.

We used for the catalog comparisons the 16-parameter transformation accounting for rotations around the three axes, a glide, and degree-2 electric- and magnetic-type deformations (see e.g., Mignard and Klioner 2012). The coordinate differences $\Delta\alpha$ and $\Delta\delta$ between a catalog and a reference catalog read

$$
\begin{aligned}
\Delta\alpha\cos\delta &= R_1\cos\alpha\sin\delta + R_2\sin\alpha\sin\delta - R_3\cos\delta - D_1\sin\alpha + D_2\cos\alpha + M_{20}\sin 2\delta \\
&+ \left(E_{21}^{\mathrm{Re}}\sin\alpha + E_{21}^{\mathrm{Im}}\cos\alpha\right)\sin\delta - \left(M_{21}^{\mathrm{Re}}\cos\alpha - M_{21}^{\mathrm{Im}}\sin\alpha\right)\cos 2\delta \\
&- 2\left(E_{22}^{\mathrm{Re}}\sin 2\alpha + E_{22}^{\mathrm{Im}}\cos 2\alpha\right)\cos\delta - \left(M_{22}^{\mathrm{Re}}\cos 2\alpha - M_{22}^{\mathrm{Im}}\sin 2\alpha\right)\sin 2\delta, \\
\Delta\delta &= -R_1\sin\alpha + R_2\cos\alpha - D_1\cos\alpha\sin\delta - D_2\sin\alpha\sin\delta + D_3\cos\delta + E_{20}\sin 2\delta \\
&- \left(E_{21}^{\mathrm{Re}}\cos\alpha - E_{21}^{\mathrm{Im}}\sin\alpha\right)\cos 2\delta - \left(M_{21}^{\mathrm{Re}}\sin\alpha + M_{21}^{\mathrm{Im}}\cos\alpha\right)\sin\delta \\
&- \left(E_{22}^{\mathrm{Re}}\cos 2\alpha - E_{22}^{\mathrm{Im}}\sin 2\alpha\right)\sin 2\delta + 2\left(M_{22}^{\mathrm{Re}}\sin 2\alpha + M_{22}^{\mathrm{Im}}\cos 2\alpha\right)\cos\delta,
\end{aligned}
$$

where α and δ are the coordinates of the object in the reference catalog. We used weighted least-squares to solve the system, with weights computed using the available covariance information (i.e., the standard errors on individual source coordinates and their correlation). The values of the transformation parameters adjusted to the catalogs compared

to the ICRF2, the ICRF3X and Gaia DR2 and their standard errors are reported in Figure 4. The resulting statistics after removal of systematics are reported in Table 2. Figure 4 reveals that the results are similar independently from the set of sources used for the comparisons. The comparisons with ICRF2 show the presence of significant deformations, particularly D3 and E20, associated to the purely zonal deformations in $\cos\,\delta$ and $\sin\,2\delta$, respectively, along the polar axis of the celestial frame. These deformations range between 10 and 80 μas depending on the individual solution. The analysis of the transformation onto ICRF3X shows that the only remaining significant deformations are those represented by D2 and D3; their values suggest that an offset between the equators of ICRF2 and ICRF3 could be the origin of this deformation. The transformation parameters with respect to Gaia DR2 show the presence of a rotation, certainly due to the fact that the individual VLBI solutions have been aligned to ICRF2 and Gaia's frame has been oriented onto ICRF3. Also deformations are visible dependent on declination, confirming the curves in Figure 2, right.

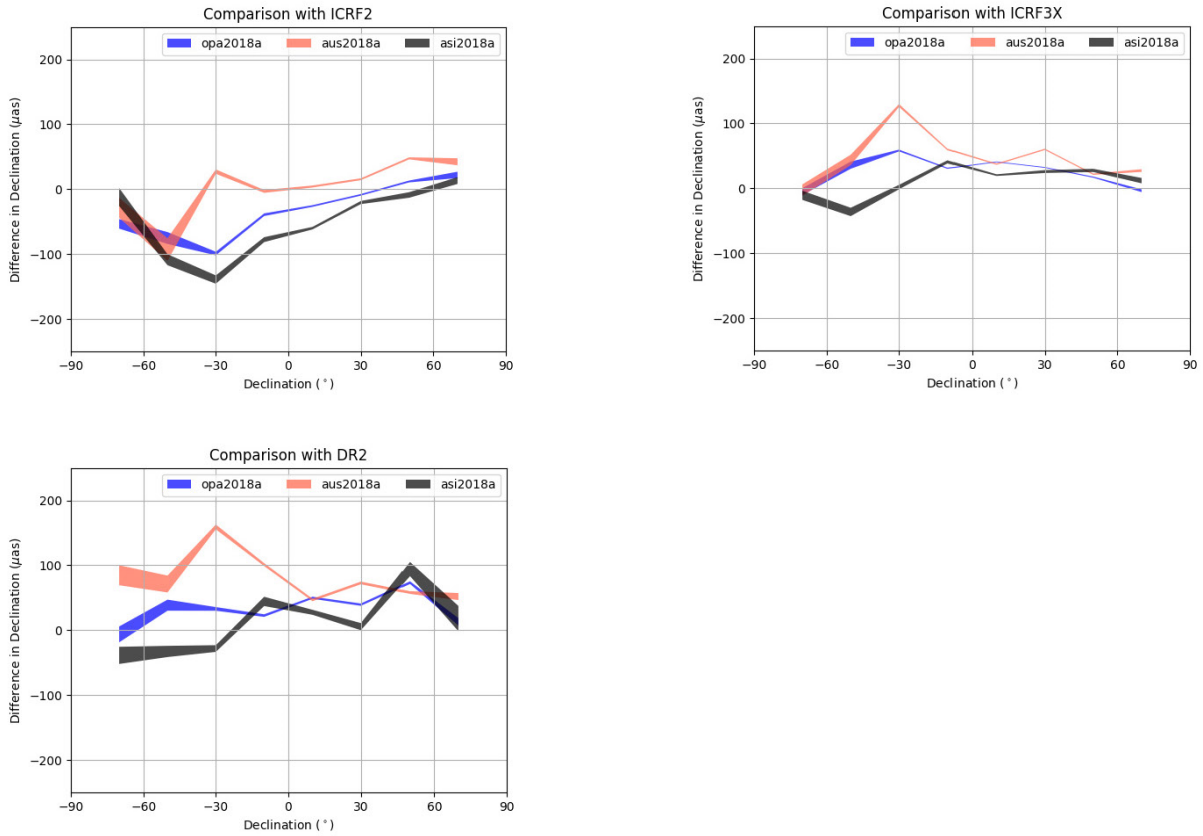

Fig. 3: *Differences in declination between the catalogs and the references (ICRF2: top left; ICRF3X, top right; Gaia DR2, bottom) averaged in bins of declination of width 15 °.*

Table 2: *Statistics of the differences of the catalogs to ICRF2, ICRF3X and Gaia DR2 with different sets of common sources, and after removal of large-scale systematics. RA* stands for RA cos_dec. Unit is μas.*

2a. With respect to ICRF2, N: number of sources common in ICRF2 and each individual catalog.

	N	Std_RA*	Std_Dec	Chi2_RA*	Chi2_Dec	Std_RA*	Std_Dec	Chi2_RA*	Chi2_Dec
opa2018a	3398	103.39	123.15	0.63	0.62	102.20	118.45	0.62	0.57
aus2018a	3359	124.76	146.58	0.71	0.70	124.46	145.09	0.71	0.68
asi2018a	893	96.73	122.20	1.57	1.87	91.27	110.24	1.40	1.52

2b. With respect to ICRF2, N: number of ICRF2 defining sources common in ICRF2 and each individual catalog.

	N	Std_RA*	Std_Dec	Chi2_RA*	Chi2_Dec	Std_RA*	Std_Dec	Chi2_RA*	Chi2_Dec
opa2018a	295	53.43	72.62	0.89	1.28	50.36	62.28	0.79	0.94
aus2018a	294	64.31	80.18	1.08	1.33	63.42	75.66	1.05	1.19
asi2018a	295	73.19	92.90	1.60	2.04	64.24	73.42	1.23	1.27

2c. With respect to ICRF2, N: number of sources common to all catalogs.

	N	Std_RA*	Std_Dec	Chi2_RA*	Chi2_Dec	Std_RA*	Std_Dec	Chi2_RA*	Chi2_Dec
opa2018a	727	62.76	82.07	0.76	0.96	60.61	73.90	0.71	0.78
aus2018a	727	86.84	101.77	1.15	1.19	86.36	99.84	1.14	1.14
asi2018a	727	94.45	119.26	1.61	1.94	88.44	105.94	1.41	1.53

2d. With respect to ICRF3X, N: number of sources common in ICRF3X and each individual catalog.

	N	Std_RA*	Std_Dec	Chi2_RA*	Chi2_Dec	Std_RA*	Std_Dec	Chi2_RA*	Chi2_Dec
opa2018a	4149	89.76	90.13	1.02	0.75	77.10	85.25	0.75	0.67
aus2018a	4234	117.42	127.78	1.07	1.01	107.53	121.35	0.89	0.91
asi2018a	941	64.11	70.28	1.63	1.67	57.91	66.81	1.33	1.51

2e. With respect to ICRF3X, N: number of ICRF3 defining sources common in ICRF3X and each individual catalog.

	N	Std_RA*	Std_Dec	Chi2_RA*	Chi2_Dec	Std_RA*	Std_Dec	Chi2_RA*	Chi2_Dec
opa2018a	303	51.13	37.52	1.52	0.71	23.39	24.00	0.32	0.29
aus2018a	300	61.85	62.67	1.66	1.51	39.76	45.27	0.69	0.79
asi2018a	273	46.65	47.30	1.28	1.17	38.55	42.17	0.87	0.93

2f. With respect to ICRF3X, N: number of sources common to all catalogs.

	N	Std_RA*	Std_Dec	Chi2_RA*	Chi2_Dec	Std_RA*	Std_Dec	Chi2_RA*	Chi2_Dec
opa2018a	727	56.28	43.87	1.55	0.78	31.16	32.51	0.48	0.43
aus2018a	727	72.74	73.05	1.80	1.55	54.31	60.33	1.00	1.05
asi2018a	727	60.66	67.34	1.65	1.74	53.54	63.62	1.28	1.55

2g. With respect to Gaia-DR2, N: number of sources common in DR2 and each individual catalog.

	N	Std_RA*	Std_Dec	Chi2_RA*	Chi2_Dec	Std_RA*	Std_Dec	Chi2_RA*	Chi2_Dec
opa2018a	2781	297.77	318.88	2.30	2.23	296.66	315.79	2.29	2.19
aus2018a	2816	344.25	358.40	1.89	1.68	342.91	355.05	1.87	1.65
asi2018a	775	218.50	222.77	2.47	2.65	214.37	218.13	2.38	2.54

2h. With respect to Gaia-DR2, N: number of sources common to all catalogs.

	N	Std_RA*	Std_Dec	Chi2_RA*	Chi2_Dec	Std_RA*	Std_Dec	Chi2_RA*	Chi2_Dec
opa2018a	727	209.01	218.12	2.60	2.80	207.00	212.41	2.55	2.66
aus2018a	727	230.90	239.01	2.53	2.58	228.00	232.25	2.47	2.43
asi2018a	727	211.60	219.81	2.42	2.70	207.84	214.90	2.34	2.58

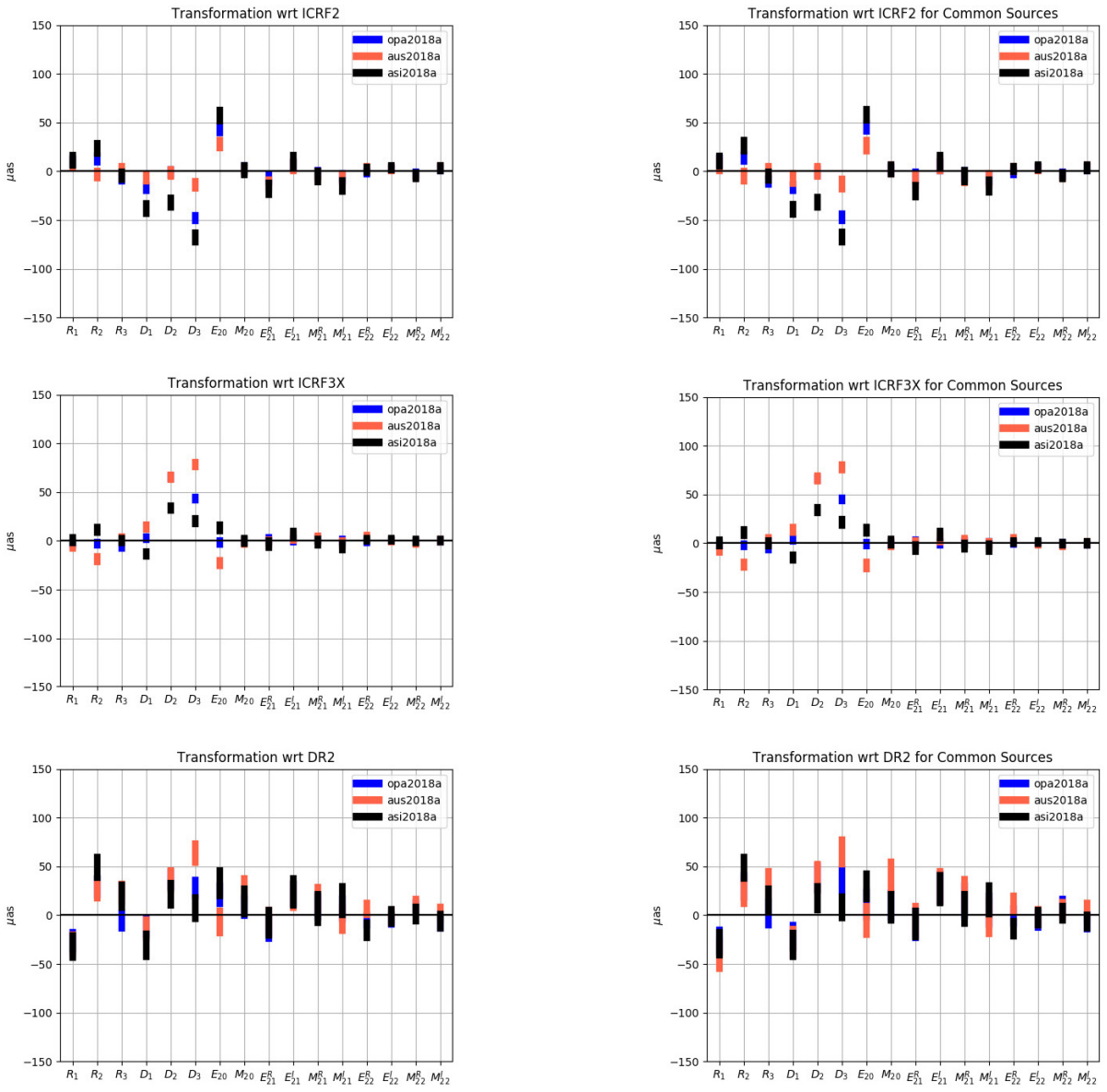

Fig. 4: *Transformation parameters between the catalogs under analysis and the reference frames (ICRF2: up, ICRF3X: middle, Gaia DR2: down). The plots on the left represent parameters computed with sources common to each individual catalog and the frame used as reference (from top to bottom they correspond to the statistics in tables 2a, 2d and 2g); the plots on the right represent parameters computed with sources common to all the catalogs involved in the comparisons, including the references (from top to bottom they correspond to the statistics in tables 2c, 2f and 2h).*

Galactic aberration has been accounted for in the computation of ICRF3X source positions. A part of the detected zonal differences between ICRF3X and Gaia DR2 and the three analyzed catalogs is imputable to the uncorrected Galactic aberration that moves sources towards the Galactic center following a glide of amplitude close to 5 μas/yr (e.g., Kovalevsky 2003; Titov et al. 2011). Considering that the epochs of ICRF3 and Gaia DR2 are close (2015.0 and 2015.5 respectively), this

effect is expected to be of around 30 μas in D_2 and D_3 for the epochs of the individual catalogs (around 2009), explaining part of the results.

Conclusions and recommendations

Three individual catalogs submitted to the IVS in 2018 are analyzed in this report. The axes of their frames are consistent with ICRF2 (to which they have been aligned) at the level of 30 μas except for zonal deformations in cos δ and sin 2δ for which the amplitude of the difference reaches about 70 μas (likely a combination of effects including the Galactic aberration and a network improvement). Compared to ICRF3X their axes are consistent to less 10 μas, but zonal deformations in cos δ peaking around 70 μas are present. All three catalogs are consistent with Gaia DR2 within μas.

For a better evaluation of the consistency of the VLBI products and a better maintenance of the reference frame, we encourage analysis centers to submit solutions aligned to the new reference ICRF3. These catalogs should be as complete as possible, i.e., processing as much VLBI sessions as possible since 1979. Analysis strategies should be rigorously documented and motivated. The main points that will be scrutinized in the next reports will be the zonal systematics, their relation with the Galactic aberration, and the agreement with the current (DR2) and future releases of Gaia.

Validation of the Gaia catalogue in the CU9

The Gaia mission goal is to create an extraordinarily precise three-dimensional map of about one billion stars throughout our Galaxy and beyond. The Gaia mission through its successive releases delivers an astronomical catalogue and data archive of unprecedented scope, accuracy and completeness. A large pan-European team of expert scientists and software developers known as DPAC (Data Processing and Analysis Consortium) is responsible for the processing of Gaia's data with the final objective of producing the Gaia Catalogue. Coordinated by the DPAC Executive, the consortium is sub-divided into nine smaller, specialist units known as Coordination Units, or CUs, with each unit being assigned a unique set of data processing tasks.

Some members of the ICRS Centre belong to the CU9/WP944 group, responsible for validation of Gaia Catalogue Data Release with the validation Test Report. The aim of these tests is to check that Gaia data is coherent compared to other known catalogues, so to accept or not them for publication. In 2018, we have updated external catalogues files, tests code and reports (VTS 060) to validate QSO and AGN which will be included in the next Gaia Catalogue Data Release DR3. These tests include rotation, cross-matching and completeness of these sources compared with QSO and AGN from external catalogues. The external catalogues used are ICRF3, LQAC-5, GIQC, SDSS DR14Q, specific catalog as AGN's in Extended Sources Catalog where the class

probability for QSO and AGN is well defined. Other large catalogues are involved, as MilliQuas and unWISE Data.

In the following we show some results of our VTS:

LQAC4GMAG cross-matched with GAIA DR2 (VTS_060_01)

.

```
Crossmatch radius:        1.0 arcsec
Crossmatched size and
percentage:               323 774 / 443 725 : 73%
Not found in Gaia:        127 238 / 443 725 : 29%
Multiple cross matches:   7 230 / 323 774 :   2 %
NonDuplicated Sources:    309 257/443 725  : 70%
NaN or 0 values in Gaia data need
for VTS: 0/323774 : 0.0%

Rotation between ICRF3 and GAIA DR2(VTS_060_04):

Rotation angles R1 R2 R3, Deformation D1 D2 D3,
with respective errors, in µas

  R1      R2      R3       D1      D2       D3
13.18   -7.94    0.23    62.42  -69.84  -147.31

 σ_R1    σ_R2    σ_R3    σ_D1    σ_D2    σ_D3
26.92   25.79   23.98   25.73   24.51   25.71
```

Study of the quasars with the Gaia DR2

Gaia Data Release 2 (GDR2) contains more than 550,000 quasars (Mignard et al. 2018). This number comes from the cross matching to bona fide quasars repositories as allWISEagn (Assef et al. 2018) and the LQAC-4 (Gattano et al. 2018), providing that the matched sources have zero proper motion and parallax as computed from Gaia sequence of measurements. And yet the direct comparison of the GDR2 to other, denser quasar repositories, as the Gaia Initial Quasar Catalog (Andrei et al. 2014) and the MilliQuas (Flesch 2017), leaves out as many as 50% of that number (Liao et al. 2018) or more, within the range of Gaia observable magnitudes. The discrepancy arguably arises because of morphological issues as optical jets and emitting blobs along the jets, or magnitude variability which can be associated to transient changes of the photocenter or simply deterioration of its determination due to photon noise. As a result spurious proper motion or even parallax can turn up, and the quasar would not at principle be shorthanded as such.

N. Liu et al. (2018) investigate the systematic errors in the very long baseline interferometry (VLBI) positions of extragalactic sources (quasars) and the global differences between Gaia and VLBI catalogs, using the GDR1 positions as the reference and study the positional offsets of the second realization of the International Celestial Reference Frame (ICRF2). They select a sample of 1032 common sources among the catalogs and adopt two methods to represent the systematics: considering the differential orientation (offset) and declination bias; analyzing with the vector spherical harmonics (VSH) functions.

They find that: the significant declination bias between Gaia DR1 and ICRF2 catalogs reported in previous studies is possibly attributed to the systematic errors of ICRF2 in the southern hemisphere. It declination-dependent systematics may exist in the VLBI positions, to need further investigations in the future Gaia data release and the next generation of ICRF.

Also, there is great interest in building unbiased catalogues of quasars for a range of important astrophysical questions. These include understanding the quasar phenomenon itself and the growth and occurrence of supermassive black holes through cosmic time, the use of quasars as probes of intervening material and their role in in re-ionization of both hydrogen and helium, and for the UV background levels throughout the universe. Thus the more diverse are the ways to assert a quasar amid the Gaia data releases, the less biased is the approach to those astrophysical questions. Conversely, the most varied are the means employed for the analysis, the largest is the sureness on the answers and the best becomes the chance to spot interesting objects or spurious detections.

In the frame of the ICRS Centre activities, Andrei et al. (2019) used observational data to check the power of the Maximum Entropy Principle on finding the behavior of the luminosity function of quasars. They carry out statistical tests showing the evaluation of the results. Even from limited observational information, over the number of quasars with a certain magnitude, at a given redshift, they find the probability for all values of the luminosity in that redshift from the principle. In this work we do not assume any specific luminosity function of the quasars. The research concludes that that the approach from the Maximum Entropy Principle leads to make estimates outside observational limits. The method therefore is promising when applied on large scale over the Gaia quasars data releases, either to check the luminosity function itself and its extension beyond the Gaia range of magnitudes, as well as an alternative method to spot outliers.

Construction of the LQAC-5 catalogue

In the frame of the ICRS Centre and during the whole year 2018, we constructed the fifth release of the Large Quasar Astrometric Catalogue. Since the previous release LQAC-4 (Gattano et al. 2018), a large number of quasars have been discovered, in particular those coming from the last release DR14Q of the SDSS. Moreover, for cross-matched objects, we have taken advantage of the very accurate determinations of the quasars identified within the recent Gaia DR2 catalogue. Following the same procedure as in the three previous release LQAC-4, we have compiled the large majority of all the objects fully reckoned as quasars (from their redshift and absolute magnitude) recorded so far. Our goal was to record their best coordinates and substantial information

concerning their physical properties such as the redshift as well as multi-bands apparent and absolute magnitudes. Emphasis was given to the results of the cross-matches with the recent Gaia DR2 catalogue.

New quasars coming from the DR14Q release were cross-matched with the previous LQAC-4 compilation with a 1″ search radius, in order to add the objects without counterpart to the LQAC-4. A similar cross-match was done with Gaia DR2 to identify the known quasars detected by Gaia. Thus, we could improve significantly the positioning of these objects, and in parallel we could study the astrometric quality of the individual catalogues of the LQAC-5 compilation. Finally, a new method was used to determine absolute magnitudes.

The LQAC-5 (Souchay et al. 2019) contains 592 809 objects. This is roughly 34% more than the number of objects recorded in the LQAC-4. Among them, 398 697 quasars were found in common with the Gaia DR2, with a 1″ search radius. That corresponds to 67.26% of the whole population in the compilation. The LQAC-5 delivers to the astronomical community a nearly complete catalogue of spectroscopically confirmed quasars (including a small proportion of compact AGNs), with the aim of giving their best equatorial coordinates with respect to the ICRF2 and with exhaustive additional information. For more than 50% of the sample, these coordinates come from the very recent Gaia DR2. The LQAC-5 catalog is available at the CDS via anonymous ftp to http://cdsarc.u-strasbg.fr.

Search for systematics effects on the tie between the Gaia and VLBI realizations of the CRF

Because of the coincident astrometric progress brought by the Gaia intermediate catalogues (and the final one within the next three years), and by the adoption of the ICRF3 as well as with the forthcoming higher frequencies CRF realizations, much effort has been conveyed into studying the systematics of the radio and optical definitions of the celestial frame.

In the frame of the ICRS Center, Taris et al. (2018) describe the magnitude variations of 47 targets that are suitable for the link between the Gaia and VLBI reference systems. They conclude that if the coordinates of the targets were affected by a white-phase noise with a formal uncertainty of about 1 mas it would affect the precision of the link at the level of 50 μas. J.-C. Liu et al. (2018) investigate the systematic errors in VLBI positions of quasars and the global differences between Gaia DR1 and the ICRF2 using 1032 common sources to find a significant declination bias attributed to the systematic errors originating from the ICRF2 in the southern hemisphere. They remarked that a comparison of the VLBI and Gaia proper motions shows that the accuracies of the components of rotation and glide between the two systems are 2–4 μas/yr, based on about 600 common sources. Abellán et al. (2018) have studied a complete radio sample of active galactic nuclei

with the VLBI technique and for the first time successfully obtained high-precision phase delay astrometry at Q band (43 GHz). They found that discrepancies arise in the orientation of the core-shifts determined through the different methods. In some cases the discrepancies could be explained by curvatures in the jets and departures from conical jets. Voitsik et al. (2018) present of a pilot project with the participation of the "Kvazar-KVO" radio interferometry array in observations carried out with the European VLBI Network. The aim of the project was to conduct and analyze multi-frequency (1.7, 2.3, 5.0, 8.4 GHz) observations of the parsec-scale jets of 24 active galactic nuclei. Mignard et al. (2018) remark that the Gaia DR2 contains the astrometric parameters for more than half a million quasars. This set defines a kinematically non-rotating reference frame in the optical domain and a subset with accurate VLBI positions allows the axes of the reference frame to be aligned with the ICRF.

Gattano et al. (2018) present the LQAC-4, which contains 443,725 objects, and for more than 50% of the sample accurate coordinates are found in the GDR1. Paine et al. (2018) present an all-sky sample of 567,721 AGNs in GDR1, selected using WISE two-color criteria. The catalog has fairly uniform sky coverage beyond the Galactic plane, with a mean density of 12.8 AGNs per square degree. Guo et al. (2018) used a near-zero proper motion criterion in conjunction with WISE [W1-W2] color to select quasar candidates, and as a result they present a catalog of 662 753 quasar candidates, with a completeness of about 75% and a reliability of 77.2%.

Photometric follow-up of QSO's from the ICRF

One of the key programs of the ICRS Centre is the photometric follow-up of QSOs which are very time consuming due to the very large amount of ICRF targets to monitor. Generally, these programs are done in the frame of international calls for proposal. This last point could be an issue when the total observation time requested is important. To avoid these constraints the SYRTE department of Paris Observatory planned to build a robotic telescope dedicated to the monitoring of QSOs magnitudes. The first part of this project began in 2015 by the choice of a site with a good atmosphere, characterized by its seeing. We chose Saint-Véran (altitude 3000m), in the French Alps, near the Italian border, for implementing a site seeing monitoring campaign (http://stveran.obspm.fr/index.php?page=statistiques). This site is known since 1960 when France initiated a site search campaign to build a 4m telescope. The goal of our campaign is to show, with modern instruments, that the site seeing, together with the number of clear nights in a year, is effectively the expected one.

Thus, it has been demonstrated in 2016 that the median value of the seeing is 1″ (mode seeing is 0.7″) which made this site a very good

one, probably one of the best in Europe. These measurements were obtained with a commercial apparatus, covered by a Non-Disclosure Agreement. The quality of the measurements was hence compared against the ones obtained by a DIMM telescope. The clear nights represent approximately 50% of the year, this amount being obtained by an AllSky camera which is able to count the visible stars in the sky every minute.

In the second step of this project, the SYRTE laboratory proposed to robotize a test telescope (0.50m) already on site since 2015. It is owned by a French amateur astronomers association, AstoQueyras. The goal of this part of the project is to show that it is possible to operate a telescope remotely from Paris in an “extreme” site. This second part of the project began in 2017 by the automation of the instrument. The first “remote light” was obtained from Paris Observatory on the January 23rd, 2018. Another “first remote light” was obtained by amateur astronomers on April 15th, 2018. During the year 2018 other tests were performed in order to check the entire configuration of the telescope, including dome, remote software control, etc. In September 2018 the concrete pillar for the scheduled 1m telescope was built. In parallel with these tests, the year 2018 was also the funding dossier creation phase of the 1m telescope, dossier that will be submitted in 2019.

Naval Observatory IERS ICRS Centre Activities During 2018

USNO concentrated on eight primary areas of work in support of maintenance and improvement of the Celestial Reference Frame:

1. Support to the International Celestial Reference Frame-3 (ICRF3) working group in the development and release of ICRF3
2. Completion of the USNO Robotic Astrometric Telescope (URAT) nearby stars and bright stars southern hemisphere surveys
3. Development and deployment of the Deep South Telescope (DST) at Cerro Tololo Interamerican Observatory (CTIO)
4. Execution of a deep, Near InfraRed (NIR) survey in the northern hemisphere using the United Kingdom Infrared Telescope (UKIRT)
5. Management of ICRS/ICRF observations utilizing the Very Long Baseline Array (VLBA)
6. Development, jointly with Paris Observatory, of the Fundamental Reference AGN Monitoring Experiment (FRAMEx)
7. Improving the astrometry of AllWISE with Gaia results
8. Use of machine-learning to identify possible reference frame AGN in NIR data along the galactic plane

ICRF3

USNO participated as a member of the IAU-sanctioned ICRF3 Working Group. Work included support for the execution and analysis of VLBA Calibrator Survey (VCS)-type Very Long Baseline Array (VLBA) S/X-band observing sessions under USNO's 50% timeshare agreement with the National Radio Astronomy Observatory (NRAO) and support for VLBA K-band and X/Ka band observations as ICRF3 sources (see below for details). Work also included generation and analysis of numerous ICRF3 prototype global VLBI solutions for comparison with those generated by other ICRF3 Working Group members at different Very Long Baseline Interferometry (VLBI) analysis centers. USNO has continued to expand the Radio Reference Frame Image Database (RRFID), a Web accessible database of radio frequency images of ICRF sources, which is available at http://rorf.usno.navy.mil/rrfid.shtml. ICRF3 was adopted by the IAU at its XXXth General Assembly in August 2018 and has replaced the previous realization, ICRF2, on January 1, 2019 (Charlot et al. 2020).

URAT Nearby Stars

Using two years of USNO Robotic Astrometric Telescope (URAT) observations in combination with USNO CCD Astrograph Catalog (UCAC) 4 and Southern Proper Motion 4 (SPM4) catalog data, parallaxes of southern stars were obtained. A catalog of 916 newly discovered nearby stars with first trigonometric parallaxes was published before the Gaia DR2 release (Finch et al. 2018). This catalog significantly improved the completeness of nearby stars known to be within 25 pc of the Sun.

URAT Southern Hemisphere Bright Star Survey

While the core of optical astrometric data for the next few decades is expected to come from the Gaia mission (Mignard et al. 2018), there are limitations with Gaia. Specifically, the Gaia focal plane physically saturates at G=12 in regular observing mode. The second Gaia data release (April 2018) contains astrometric results for some stars in the 3.5 to 6 magnitude range, observed with special "bright star modes". However, at this point it is unclear if and when the Gaia project will be able to release accurate results for all bright stars.

In order to address this gap in the optical reference frame, USNO continues with the UBAD survey at NOFS and the URAT bright star program at CTIO (see 2017 annual report). Observations with the USNO astrograph (URAT) concluded in June 2018 when the instrument was decommissioned to make room for a new program (see below). All bright stars south of declination +25 deg were observed with URAT over 2.7 years yielding typically several hundred images per star. Reductions of the data for both UBAD and URAT continued throughout the calendar year 2018. Release of an integrated bright star catalog covering all bright stars, and aligned to the Gaia reference frame, is expected in

2020.

Deep South Telescope (DST) A fraction of ICRF sources (about 10%) display abnormally large optical vs. radio position differences when comparing Gaia results with VLBI data. In order to investigate this further, USNO acquired a new 1-meter telescope to be deployed at Cerro Tololo Interamerican Observatory (CTIO) in Chile. This Deep South Telescope (DST) was built by PlaneWave Instruments in 2018 and first light was obtained in December at the PlaneWave factory near Los Angeles in California (see Figure 5).

A 4k by 4k CCD camera has been ordered to provide a 35 arcmin field of view at 0.515 arcsec/pixel resolution. A wheel with 8 filters (wide bandpass, *B, V, R, I, g, r, i*) is on order as well. Deployment to Cerro Tololo, Chile is expected in 2019. The initial DST optical observing program aiming at about 200 selected ICRF sources with high cadence observing is part of a new joint USNO/Paris Observatory collaboration (FRAMEx, see below for more information).

Fig. 5: *DST (model PW1000) at PlaneWave Instruments, Compton, CA, USA, December 2018. As shown, DST telescope is undergoing acceptance testing.*

USNO UKIRT K-Band Hemispherical Survey

USNO, in collaboration with the Institute for Astronomy (IfA) at the University of Hawaii (UH); the School of Physics and Astronomy, Nottingham University; Institute of Astronomy, University of Cambridge; and the Institute for Astronomy, University of Edinburgh, continued a K-band multi-year, northern hemisphere survey in the Near InfraRed (NIR) using the United Kingdom Infrared Telescope (UKIRT). This survey is targeted for completion in the 2021 time frame. When completed, the K-band survey will provide a catalog to fainter than 18th magnitude that complements the VISTA Hemisphere Survey in the southern hemisphere (McMahon 2013).

When combined with the J-band UKIRT survey (Dye et al. 2018), the K- data will provide deep photometric and astrometric data for two of the three standard NIR astronomical photometry bands. Figure 6 shows the progress of the survey through December 2018. When incorporating K-band data from earlier, directed surveys, approximately 60% of the northern sky had been completed through the end of 2018.

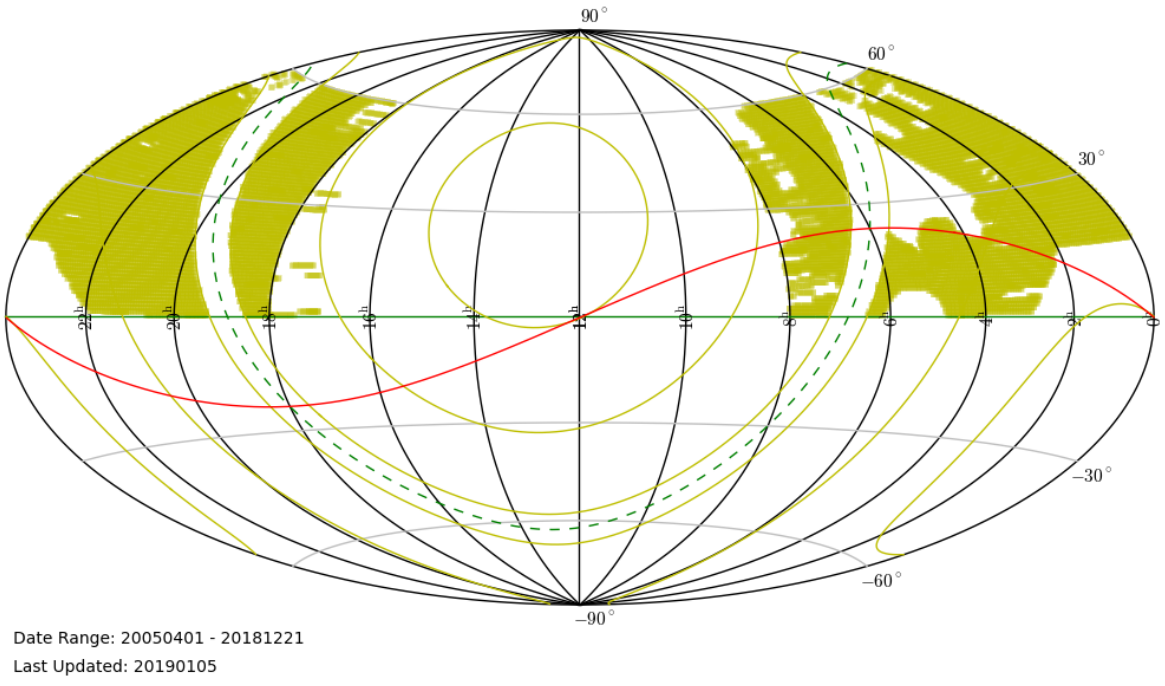

Fig. 6: *UKIRT K-band survey progress, as of Dec 2018. Note that the galactic plane and the region centered around the North Galactic Pole (RA 12 h 51′, DEC +27 deg 07′) were previously surveyed; the current survey fills in the gaps. Also note that UKIRT cannot observe above DEC +60 deg; this "polar cap" will be filled in with dedicated observations using a different telescope at a later time.*

USNO 50% timeshare of the Very Long Baseline Array (VLBA)

As described in the 2017 IERS ICRS report, USNO now schedules 50% of the observing time for the Very Long Baseline Array (VLBA), the National Science Foundation (NSF)/National Radio Astronomy Observatory (NRAO) facility that consists of ten 25-m radio telescopes that span a baseline from Hawaii in the the Virgin Islands in the east (see Figure 7). This facility is used to support astrometry of reference frame objects, geodesy, and astronomical and astrophysical research, including into reference frame objects.

During the time period 2017–2018, USNO provided a significant amount of VLBA time to the development of ICRF3. This included observations in both the S/X bands (PI: D. Gordon, NASA/GSFC) as well as K-band (PIs: A. deWitt, HartRAO; C. Jacobs, NASA/JPL). USNO-provided VLBA time improved S/X source precision by a factor of 3x or better, and provided approximately 99% of the observations that were used to develop the K-band reference frame.

Fig. 7: *Very Long Baseline Array (VLBA) Telescope located at Pie Town, New Mexico. The array consists of ten such telescopes, spanning a baseline from Hawaii in the west to the US Virgin Islands in the east.*

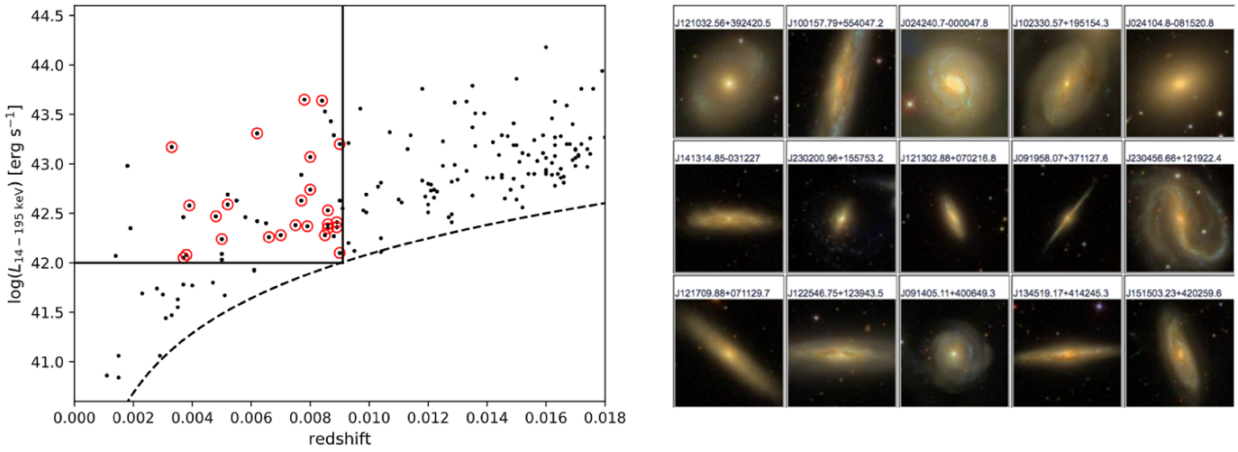

Fig. 8: *Left: luminosity limit of BAT 105-month catalog as a function of redshift, showing our volume-limited selection box. Objects circled in red are those within a declination range of -30 to +60 deg. Right: SDSS thumbnails of 15/25 of our sample.*

Fundamental Reference Frame AGN Monitoring Experiment (FRAMEx)

The Fundamental Reference AGN Monitoring Experiment (FRAMEx) was conceived at a May 2018 USNO-Paris Observatory IERS ICRS Centre meeting. The purpose of FRAMEx is to study representative samples of AGN/quasars to understand the physical processes potentially involved in optical-radio positional offsets seen in many ICRF sources. We defined two samples for study: a volume-limited sample of local AGN and a sample of quasars with significant optical-radio (Gaia-VLBI) positional offsets. Observations of the latter sample, which are being taken with the new USNO Deep South Telescope (DST; PI: Zacharias, see above) have just begun, so in the following we discuss only the volume-limited sample.

Using the Swift/BAT 105-month catalog (Oh et al. 2018), which contains a highly reliable and unbiased sample of AGN selected using hard X-rays (14—195 keV), we selected a volume-complete sample of AGN with hard X-ray luminosities above 10^{42} erg s^{-1}, which gives a distance limit of ~40 Mpc for the depth of the 105-month catalog. We further selected those objects between declinations of -30 and +60 deg for observability with the VLBA, as well as with other USNO and USNO partner assets. This resulted in 25 objects (see Figure 8).

These objects are being observed on a bimonthly basis using a portion of USNO's 50% timeshare of the VLBA to monitor for core shifts, which at the physical resolution of these nearby objects (< 1 pc) corresponds to changes in accretion structure. Simultaneous observations with the Swift X-ray Telescope (XRT) are also carried out. This allows for changes seen in non-thermal emission (i.e., radio synchrotron) to be compared to thermal emission (i.e., traced by inverse-Compton up-scattering of thermal UV accretion disk photons by the hot X-ray corona), thus providing insight into findings from optical ground-based monitoring (e.g., Taris et al. 2018). The first observation epoch has

already revealed an important result, that AGN may not follow the "fundamental plane" (FP) of black hole (BH) activity (e.g., Merloni et al. 2003) as previously inferred using lower resolution VLA observations (Figure 8, from Fischer et al. 2020). This relationship is important to multi-wavelength CRF work, as it implies a coupling of the thermal and non-thermal emission in AGN, normalized by BH mass. Any sign of decoupling, for example objects not following the FP, would potentially indicate that AGN radio and optical (the latter tracing the accretion disk emission) positions and luminosities will not necessarily be correlated, potentially introducing an additional source of scatter in CRF work.

AllWISE Revised Astrometry

Data from the Wide-Field Infrared Survey Explorer (WISE; Wright et al. 2010) have been an unexpected boon for CRF work, as the extreme sensitivity of its first three bands (3.4, 4.6, and 12-micron) to AGN-dominated objects (i.e., quasars) and deep survey coverage allowed for the creation of a large (1.4 million objects) and extremely reliable (stellar contamination < 0.04%) sample of quasars (using the AllWISE catalog; Secrest et al. 2015) that allowed for the Gaia CRF to be made non-rotating (Lindegren et al. 2018). WISE has continued to take data in its two shorter wavelength bands since its initial release, with the deepest catalog released at the beginning of 2019 (unWISE; Schlafly et al. 2019). WISE will likely continue to serve various roles in current and future CRF work, and so optimization of WISE for astrometric purposes is a worthwhile endeavor. To this end, at the 2018 USNO-Paris Observatory IERS ICRS Centre Meeting USNO suggested using Gaia as a reference catalog to revise the coordinates of the AllWISE/unWISE catalogs, which suffer from zonal errors due to the ground-based catalogs their native astrometry is based on (2MASS positions + UCAC4 proper motions). Preliminary results have been a success, with the zonal errors being largely removed (Figure 10). These results are anticipated to be published by mid-2020.

Galactic Plane QSOs

A consistent goal in the production of catalogs for CRF work is homogeneity and uniformity (see, for example, the 2017 annual report). The presence of large gaps and under-dense regions in catalogs may introduce systematics that adversely affect the quality of the CRF. For multi-wavelength (i.e., non-radio) work, the biggest such gap is the Galactic plane (GP). Gaia counterparts are scarce for AGN seen behind the GP, which can exhibit extinction well in excess of E(B–V) > 2 mag. However, future astrometric missions such as GaiaNIR (Hobbs et al. 2016) will likely detect AGN deep into the GP, and so it is important to find these AGN. Towards this goal, USNO has undertaken a novel research program that utilizes a machine learning technique to assign an AGN probability, or likelihood, based on a source's near-IR magnitudes

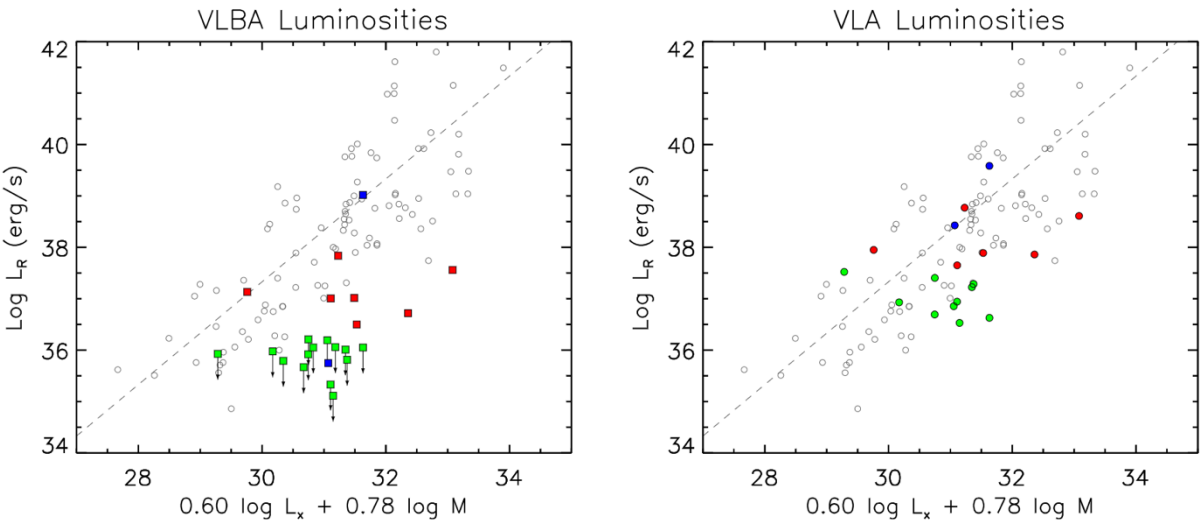

Fig. 9: *Left: distribution of our volume-limited sample on the FP (Merloni et al. 2003) using simultaneous XRT and VLBA observations. Most objects are undetected upper-limits (arrows); although many are on the FP when using lower-resolution VLA data (right).*

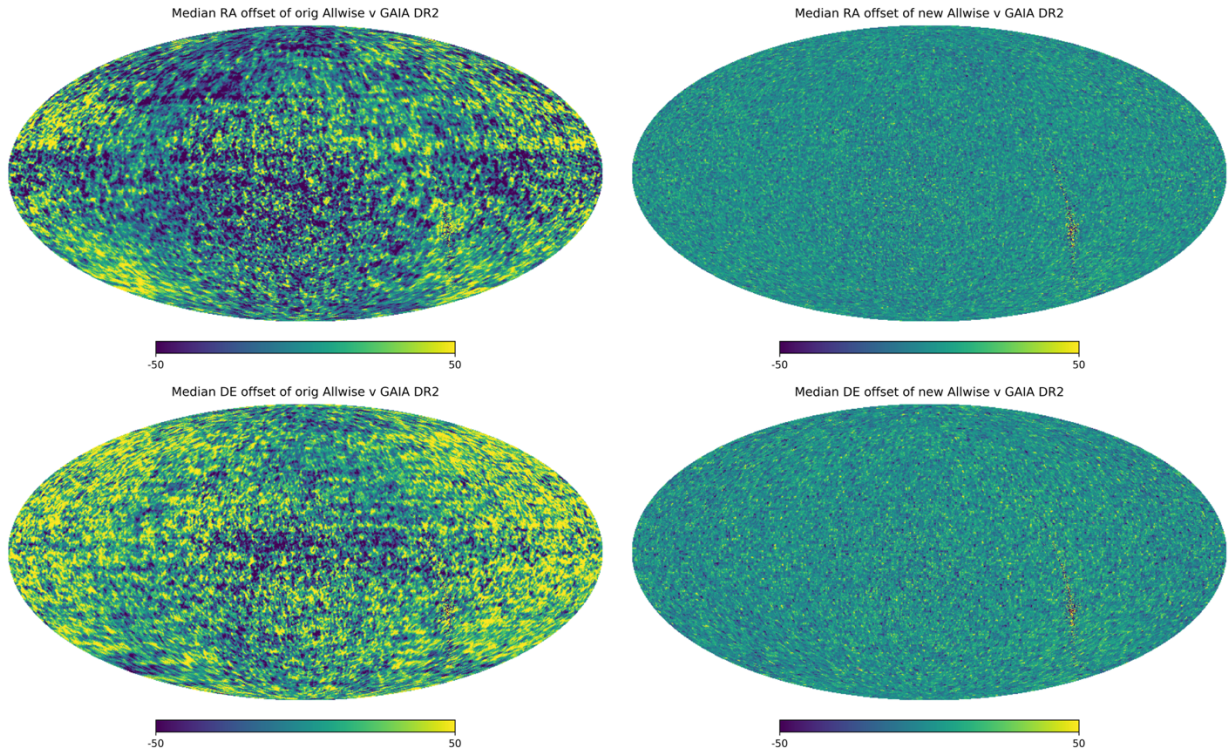

Fig. 10: *Left: median AllWISE-Gaia positional offsets in RA (top) and Dec (bottom). Right: positional offsets after astrometric re-reduction using Gaia as the reference catalog. The auxiliary axis is in units of mas.*

(*J, H, K*) as well as the known value of the Galactic extinction (e.g., Schlafly & Finkbeiner 2011) at its position and any optical counterpart it may or may not have. Preliminary results are highly promising, with the classifier performing 100 to 200 times better than random chance. USNO has an approved NIR spectroscopic program to confirm these AGN candidates using UKIRT, although logistical problems prevented any spectroscopic observations from being executed in 2018. We show our sample candidates, which so far use near-IR data from the UKIDSS GP survey (Lucas et al. 2008), in Figure 11.

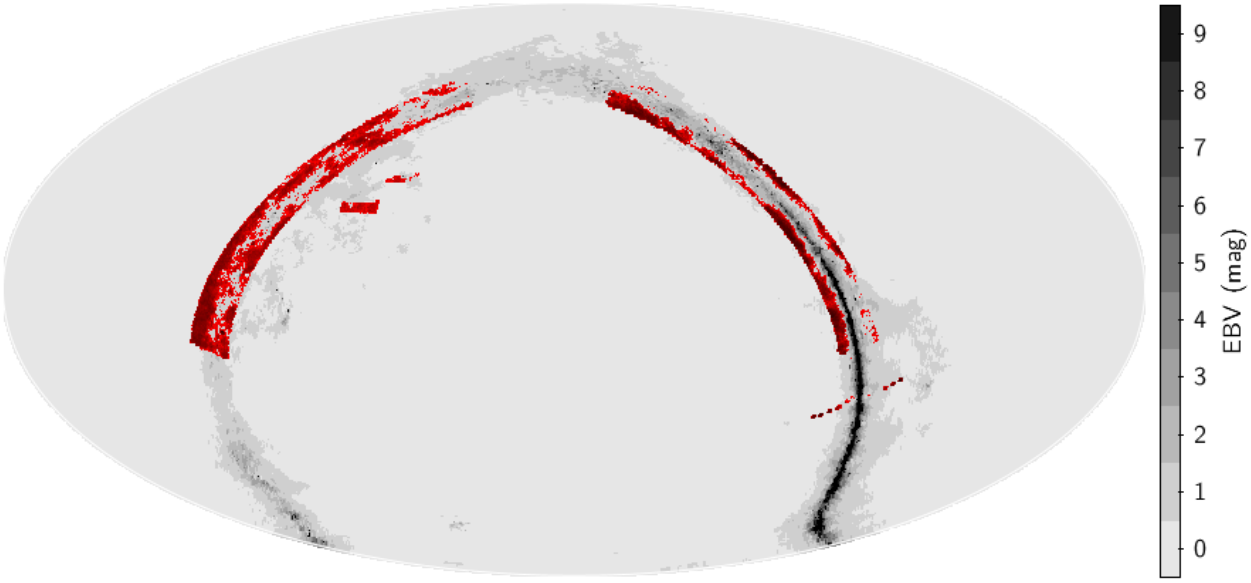

Fig. 11: *Sample of GP candidates (red) overlaid on the Galactic extinction map of Schlafly & Finkbeiner (2011), plotted in equatorial coordinates, showing AGN access deep into the GP.*

References

Abellán, F.J., Marti-Vidal, I., Marcaide, J.M. and Guirado, J.C., 2018, Astronomy & Astrophysics, 614, 74

Andrei, A.H., Antón, S., Taris, F., Bourda, G., Souchay, J., Bouquillon, J., et al., 2014, The Gaia Initial Quasar Catalog, Proc. of the Journées 2013: "Systèmes de référence spatio-temporels", Obs. de Paris, Nicole Capitaine (ed.), p. 84–87

Andrei, A.H., Coelho, B., Guedes, L.L.S., Lyra, A., 2019, The luminosity function of quasars by the Principle of Maximum Entropy, Monthly Notices of the Royal Astronomical Society, 488, 183–190

Assef, R. J., Stern, D., Noirot, G., Jun, H. D., Cutri, R. M. and Eisenhardt, P. R. M., 2018, The WISE AGN catalog, Astrophysical Journal Supplement Series, 234, 23

Brown, A.G.A., Vallenari, A., Prusti,T., et al., 2016, Gaia Data Release 1. Summary of the astrometric, photometric and survey properties. Astronomy & Astrophysics, 595, A2

Brown, A.G.A., Vallenari, A., Prusti, T., et al., 2018, Gaia Data Release 2. Summary of the contents and survey properties. Astronomy & Astrophysics, 616, A1

Charlot, P., Jacobs, C.S., Gordon, D., et al., 2020, The third realization of the International Celestial Reference Frame by very long baseline interferometry. Astronomy & Astrophysics, in preparation

Dye, S., Lawrence, A., Read, M. A., et al., 2018, The UKIRT Hemisphere Survey: definition and J-band data release, Monthly Notices of the Royal Astronomical Society, 473, 5113–5125

Fey, A.L., Gordon, D., Jacobs, C.S., et al., 2015, The Second Realization of the International Celestial Reference Frame by Very Long Baseline Interferometry. Astronomical Journal, 150, 58

Finch, C., Zacharias, N. and Jao, Wei-Chun, 2018, URAT south parallax results: discovery of new nearby stars, arXiv:1802.08272 and Astronomical Journal 155, 176F

Fischer, T. C., Secrest, N. J., Johnson, M. C., et al., 2020, Astrophysical Journal, in preparation

Flesch, E. W., 2017, CDS Vizier yCat.7280

Gattano, C., Andrei, A.H., Coelho, B., Souchay, J., Barache, C. and Taris, F., 2018, LQAC-4: Fourth release of the Large Quasar Astrometric Catalogue. Compilation of 443 725 objects including cross-identifications with Gaia DR1, Astronomy & Astrophysics, 614, A140

Guo, S., Qi, Z., Liao, S., Cao, Z., Lattanzi, M.G., Bucciarelli, B., Tang, Z. and Yan, Q.-Z., 2018, Astronomy & Astrophysics, 618, 144

Hobbs, D., Høg, E., Mora, A., et al. 2016, GaiaNIR: Combining optical and Near-Infra-Red (NIR) capabilities with Time-Delay-Integration (TDI) sensors for a future Gaia-like mission, arXiv:1609.07325

International Astronomical Union, 2019, Transactions IAU, Vol. XXXB, Proceedings of the XXX IAU General Assembly, August 2018 (Ed. Teresa Lago)

Kovalevsky, J., 2003, Aberration in proper motions. Astronomy & Astrophysics, 404, 743–747

Lambert, S.B., 2013, Time stability of the ICRF2 axes. Astronomy & Astrophysics, 553, A122

Liao, S., Bucciarelli, B., Qi, Z., et al., 2018, The properties of the quasars astrometric solution in Gaia DR2, arXiv:1805.02194

Lindegren, L., Hernández, J., Bombrun, A., et al., 2018, Astronomy & Astrophysics, 616, A2

Liu, N., Zhu, Z. and Liu, J.-C., 2018, Possible systematics in the VLBI catalogs as seen from Gaia, Astronomy & Astrophysics, 609, A19

Liu, J.-C., Malkin, Z. and Zhu, Z., 2018, Impact of quasar proper motions on the alignment between the International Celestial Reference

Frame and the Gaia reference frame, Monthly Notices of the Royal Astronomical Society, 474, 4477–4486

Lucas, P. W., Hoare, M. G., Longmore, A., et al., 2008, Monthly Notices of the Royal Astronomical Society, 391, 136

Ma, C., Clark, T.A., Ryan, J.W., et al., 1986, Radio-source positions from VLBI. Astronomical Journal, 92, 1020–1029.

McMahon, R.G., Banerji, M., Gonzalez, E., et al., 2013, First Scientific Results from the VISTA Hemisphere Survey (VHS), The Messenger, 154:35

Merloni, A., Heinz, S., & di Matteo, T., 2003, Monthly Notices of the Royal Astronomical Society, 345, 1057

Mignard, F. and Klioner, S., 2012, Analysis of astrometric catalogues with vector spherical harmonics. Astronomy & Astrophysics, 547, A59

Mignard, F., Klioner, S.A., Lindegren, L., et al., 2018, Gaia Data Release 2. The celestial reference frame (Gaia-CRF2). Astronomy & Astrophysics, 616, A14

Oh, K., Koss, M., Markwardt, C. B., et al., 2018, Astrophysical Journal Supplement Series, 235, 4

Paine, J., Darling, J. and Truebenbach, A., 2018, Astrophysical Journal Supplement Series, 236, 37

Prusti, T., de Bruijne, J.H.J., Brown, A.G.A., et al., 2016, The Gaia mission. Astronomy & Astrophysics, 595, A1

Schlafly, E.F. and Finkbeiner, D. P., 2011, Astrophysical Journal, 737, 103

Schlafly, E.F., Meisner, A.M. and Green, G. M., 2019, Astrophysical Journal Supplement Series, 240, 30

Secrest, N.J., Dudik, R.P., Dorland, B.N., et al., 2015, Astrophysical Journal Supplement Series, 221, 12

Souchay, J., Gattano, C., Andrei, A.H., Souami, D., Coelho, B., Barache, C., Taris, F., Secrest, N. and Berthereau, A., 2019, LQAC-5: The fifth release of the Large Quasar Astrometric Catalogue. A compilation of 592 809 objects with 398 697 Gaia counterparts, Astronomy & Astrophysics, 624, A145

Taris, F., Damljanovic, G., Andrei, A.H., Souchay, J., Klotz, A. and Vachier, F., 2018, Astronomy & Astrophysics, 611, 52

Titov, O., Tesmer, V. and Boehm, J., 2004, OCCAM v.6.0 Software for VLBI Data Analysis. In N. R. Vandenberg and K. D. Baver, editors, International VLBI Service for Geodesy and Astrometry 2004 General Meeting Proceedings, p. 267

Titov, O., Lambert, S.B. and Gontier, A.M., 2011, VLBI measurement of the secular aberration drift, Astronomy & Astrophysics, 529, A91

Voitsik, P.A., Pushkarev, A.B., Kovalev, Yu. Yu., Plavin, A.V., Lobanov, A.P. and Ipatov, A.V., 2018, Frequency-Dependent Core Shifts in Ultracompact Quasars. Astronomy Reports, 62, 787

Wright, E. L., Eisenhardt, P. R. M., Mainzer, A. K., et al., 2010, Astronomical Journal, 140, 1868

Bryan Dorland, Jean Souchay, Alexandre Andrei, E. Felicitas Arias, Christophe Barache, Sébastien Bouquillon, Alan Fey, César Gattano, Sébastien Lambert, Nathan Secrest, François Taris, Norbert Zacharias